Author(s): Abe, Shinya; Kouhia, Reijo; Nikander, Riku; Narra, Nathaniel; Hyttinen, Jari; Sievänen, Harri

Title: Effect of fall direction on the lower hip fracture risk in athletes with different loading histories : A finite element modeling study in multiple sideways fall configurations

Year: 2022

Version: Published version

Please cite the original version:

Abe, S., Kouhia, R., Nikander, R., Narra, N., Hyttinen, J., & Sievänen, H. (2022). Effect of fall direction on the lower hip fracture risk in athletes with different loading histories : A finite element modeling study in multiple sideways fall configurations. Bone, 158, Article 116351. https://doi.org/10.1016/j.bone.2022.116351

Bone 158 (2022) 116351

Contents lists available at ScienceDirect

Bone

journal homepage: www.elsevier.com/locate/bone

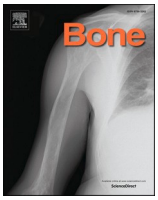

Full Length Article

Effect of fall direction on the lower hip fracture risk in athletes with different loading histories: A finite element modeling study in multiple sideways fall configurations

Shinya Abe [a,*], Reijo Kouhia [a], Riku Nikander [b,c], Nathaniel Narra [d,1], Jari Hyttinen [d], Harri Sievänen [e]

[a] Structural Mechanics, Faculty of Built Environment, Tampere University, Tampere, Finland
[b] Gerontology Research Center, Faculty of Sports Sciences, University of Jyväskylä, Jyväskylä, Finland
[c] Central Hospital of Central Finland, Jyväskylä, Finland
[d] BioMediTech Unit, Faculty of Medicine and Health Technology, Tampere University, Tampere, Finland
[e] The UKK Institute for Health Promotion Research, Tampere, Finland

ARTICLE INFO

Keywords:
Hip fracture
Bone strength
Fracture prevention
Exercise
Finite element modeling
Fall

ABSTRACT

Physical loading makes bones stronger through structural adaptation. Finding effective modes of exercise to improve proximal femur strength has the potential to decrease hip fracture risk. Previous proximal femur finite element (FE) modeling studies have indicated that the loading history comprising impact exercises is associated with substantially higher fracture load. However, those results were limited only to one specified fall direction. It remains thus unclear whether exercise-induced higher fracture load depends on the fall direction. To address this, using magnetic resonance images of proximal femora from 91 female athletes (mean age 24.7 years with >8 years competitive career) and their 20 non-athletic but physically active controls (mean age 23.7 years), proximal femur FE models were created in 12 different sideways fall configurations. The athletes were divided into five groups by typical loading patterns of their sports: high-impact (H-I: 9 triple- and 10 high-jumpers), odd-impact (O-I: 9 soccer and 10 squash players), high-magnitude (H-M: 17 powerlifters), repetitive-impact (R-I: 18 endurance runners), and repetitive non-impact (R-NI: 18 swimmers). Compared to the controls, the FE models showed that the H-I and R-I groups had significantly ($p < 0.05$) higher fracture loads, 11–17% and 22–28% respectively, in all fall directions while the O-I group had significantly 10–11% higher fracture loads in four fall directions. The H-M and R-NI groups did not show significant benefit in any direction. Also, the analyses of the minimum fall strength (MFS) among these multiple fall configurations confirmed significantly 15%, 11%, and 14% higher MFSs in these impact groups, respectively, compared to the controls. These results suggest that the lower hip fracture risk indicated by higher fracture loads in athletes engaged in high impact or repetitive impact sports is independent of fall direction whereas the lower fracture risk attributed to odd-impact exercise is more modest and specific to the fall direction. Moreover, in concordance with the literature, the present study also confirmed that the fracture risk increases if the impact is imposed on the more posterolateral aspect of the hip. The present results highlight the importance of engaging in the impact exercises to prevent hip fractures and call for retrospective studies to investigate whether specific impact exercise history in adolescence and young adulthood is also associated with lower incidence of hip fractures in later life.

1. Introduction

Bone structure and density, constituting its strength [1], adapt to prevalent mechanical loading [2,3]. Physical activity and exercise provide natural ways to apply mechanical loading to the bone. These activities largely contribute to bone strength by promoting bone formation in growth [4] and help maintain skeletal strength or slow down age-related bone loss with aging [5,6]. However, not all exercises are

* Corresponding author at: Structural Mechanics, Faculty of Built Environment, Tampere University, P.O.Box 600, FI-33014 Tampere, Finland.
E-mail address: shinya.abe@tuni.fi (S. Abe).
[1] Present address: Computing Sciences Unit, Faculty of Information Technology and Communication Sciences, Tampere University, Pori, Finland.

https://doi.org/10.1016/j.bone.2022.116351
Received 11 June 2021; Received in revised form 1 February 2022; Accepted 1 February 2022
Available online 4 February 2022

equally osteogenic and the effectiveness may vary between anatomical sites [7,8]. Animal experimental studies suggest that the effective loading types are dynamic and include sufficiently high-magnitude strains produced at high strain rate or frequencies [3,9]. For the proximal femur, finding effective exercises is highly important because of increasing social and economic burden caused by hip fractures.

Hip fracture is a major public health problem leading to high rates of disability, morbidity, and mortality in the elderly population and huge financial burden to societies [10]. Over 90% of hip fractures are caused by falls [11,12]. A typical sideways fall imposes a high impact force on the greater trochanter resulting in unusually high compressive loading on the superolateral cortex of the femoral neck [13–16], where the bone structure is inherently fragile due to substantial age-related cortical thinning [17–20]. Hence, if a specific type of exercise can increase or maintain bone strength, hip fracture risk may be decreased through this exercise. There is convincing epidemiological evidence that physical activity is associated with lower hip fracture risk in a dose-response manner [21,22]. Lower fracture risk is also confirmed in a meta-analysis of exercise randomized controlled trials (RCT) [23].

Comparing the bones between athletes and non-athletic people provides a unique opportunity to explore long-term adaptation of bones to specific exercise loading. Such studies based on dual-energy X-ray absorptiometry (DXA) have found that young female athletes with a history of high-impact (e.g., jumps generating high ground reaction forces) and/or odd-impact exercise (e.g., generating ground impact from unusual directions common in ball games like football, tennis, and squash) had greater areal bone mineral density (aBMD), bone mineral content, cross-sectional area, and section modulus at the femoral neck compared to non-athletic female controls [24–28]. Our previous study based on magnetic resonance imaging (MRI) [29] has shown that the cortical bone around the femoral neck cross-section was distributed differently in athletes representing different sports: long-term high-impact and odd-impact exercises were associated with ~20% thicker cortical bone around the femoral neck including the vulnerable superolateral region. Subsequently, we have created proximal femur finite element (FE) models utilizing the same MRI data in a sideways fall configuration to examine whether the exercise-induced benefits at the athletes' femoral neck could translate into reduced fracture risk [30,31]. It was found that the proximal femur subjected to not only high-impact and odd-impact exercises, but also repetitive impact loading (e.g., endurance running) had significantly higher fracture loads suggesting the lower fall-induced fracture risk compared to the controls [30,31]. However, in these previous studies, our FE analyses were limited only to a single sideways fall direction. Since the athletes' bones are adapted to long-term exercise loading characterized by specific magnitude, rate, frequency, and direction, it remains unclear whether the exercise-induced higher fracture load is specific to only certain fall directions.

Previous experimental or FE modeling studies of multiple fall configurations have confirmed the following points: 1) fracture loads vary depending on the fall directions [32–36]; 2) fall-induced strain distributions within the loaded bone structure differ depending on the fall directions [14,37]; and 3) the simulation of multiple fall configurations is essential for evaluating the ability of FE-derived hip strength to predict the actual hip fracture occurrence in clinical applications [34–36,38–40]. However, to the present authors' knowledge, no study so far has addressed whether the exercise-induced gains in the proximal femur strength persist regardless of the fall direction or whether they are fall-direction specific. Furthermore, since falling is an unpredictable event, it is difficult to predict its direction and the weakest fall orientation is likely femur-specific. Therefore, a concept of a minimum fall strength (MFS) among the multiple fall conditions, indicating the lowest fracture load, has been recently proposed as a more advantageous variable to predict the hip fracture risk [35,40]. In fact, Falcinelli et al. [35] and Qasim et al. [40] reported that MFS can identify the actual hip fracture cases more accurately than the fracture load in a single specific fall direction or proximal femur aBMD.

The present study was therefore undertaken to expand our previous FE studies of the proximal femur in young adult female athletes and their controls [30,31] by simulating multiple sideways fall configurations. The primary objective was to evaluate whether and how the high femoral strength attributed to the specific exercise loading history depended on the fall direction. The secondary objective of the present study was to investigate whether the minimum fall strength among the multiple fall configurations differed between the exercise loading groups and their controls.

2. Materials and methods

2.1. Study participants

Proximal femur MRI data of 91 adult female athletes (aged 24.7 ± 6.1 years), competing actively at national or international level, and 20 habitually active female controls (aged 23.7 ± 3.8 years) were obtained from our previous study [29]. According to our standard exercise classification scheme [24,41], the athletes were divided into five different groups based on the typical loading patterns of their sports: high-impact (H-I) (9 triple- and 10 high-jumpers); odd-impact (O-I) (9 soccer and 10 squash players); high-magnitude (H-M) (17 powerlifters); repetitive-impact (R-I) (18 endurance runners); and the repetitive, non-impact group (R-NI) (18 swimmers). The controls indulged in recreational exercise 2–3 times a week but had never taken part in any sport at a competitive level. The study protocol was approved by the Ethics Committee of the Pirkanmaa Hospital District, and written informed consent was obtained from each participant.

Body height and weight (BW) were measured in light indoor clothing without shoes with standard methods. The body fat-% and lean body mass (LM) were measured with DXA (GE Lunar Prodigy Advance, Madison, WI, USA). Questionnaires were completed by all participants to obtain their training history including weekly sport-specific training hours and the number of training sessions during at least five preceding years [29].

2.2. MRI scanning procedure

Participants' hip regions were scanned using 1.5-T MRI system (Avanto Syngo MR B15, Siemens, Erlangen, Germany). The scanned hip region volume covered the proximal femur from the top of the femoral head to the subtrochanteric level of the femoral diaphysis. The imaging sequence was a standardized axial T1-weighted gradient echo volumetric interpolated breath-hold (VIBE)-examination with the following parameters: FOV 35 × 26 cm, TR 15.3 ms, TE 3.32 ms, in-plane resolution (pixel size) 0.9 mm × 0.9 mm, slice thickness 1 mm without gaps, echo train length = 1, flip angle = 10°, matrix 384 × 288. With two half-Fourier acquisition single-shot turbo spin-echo localization series, sagittal, axial, and coronal images of the hip region of the dominant side were scanned. The reconstructed imaging plane was adjusted so that the cross-sectional plane of the femoral neck was perpendicular to the femoral neck axis [29].

2.3. FE modeling and multiple sideways fall simulation

The procedure for creating the proximal femur FE models from the MRI data is described in detail elsewhere [30,31]. In short, the proximal femur MRI data were first manually segmented by delineating the periosteal and endocortical boundaries of cortical bone [42]. For the present study, the effect of segmentation error on the estimated fracture load was evaluated by re-segmenting MRI data from 12 randomly selected proximal femora, two from each group. Root-mean-square coefficient of variation (RMS-CV) and mean CV were calculated as indices of intra-operator reproducibility. The present 2.3% RMS-CV was comparable to RMS-CV of 1.9–3.6% for duplicate scans reported elsewhere [43,44]. In these two studies, the in-plane image resolution was similar

to the present study. The present 0.9% mean CV was higher than the 0.23% CV for the yield strength in a recent MRI based study [45]. This difference was likely due to ~4 times higher in-plane image resolution (0.234 mm × 0.234 mm) compared to ours (0.9 mm × 0.9 mm). Nonetheless, the present re-segmentation error was considered marginal to evaluate the expectedly much higher between-group differences in the fracture load.

After the segmention, the proximal femur geometries were converted into a volume mesh, which surface was smoothed using a method by Taubin [46]. Then, the 3D solid bodies of the proximal femur were created in SolidWorks (SolidWorks Corp., Waltham, MA, USA) before importing them into ANSYS (ANSYS Inc., Houston, PA, USA) for FE meshing and analysis.

The cortical and trabecular bone tissues in the proximal femur were modeled as homogeneous isotropic, linear elastic materials with Young's moduli of 17 GPa [47–49] and 1500 MPa [47,49], respectively. Poisson's ratio was assumed as 0.33 for all materials [47–49]. Similar cortical modulus (~15–20 GPa) was also reported for the adult population aged 22–61 years [50] and thus the choice of 17GPa was considered appropriate for the present study. As regards the trabecular modulus, Sylvester and Kramer [51] compared recently their homogeneous proximal femur FE models to the experimental data of Cristofolini et al. [52] and concluded that the modulus of the entire trabecular compartment of the proximal femur likely varies between 500 MPa and 1500 MPa.

A total of 12 different sideways fall configurations were created for each of the 111 proximal femur FE models by increasing the hip adduction angle α (an angle between the femoral shaft and the ground) in steps of 10° (0°, 10°, 20°, and 30°) and the internal rotation angle β of the femoral neck in steps of 15° (0°, 15°, and 30°) (Fig. 1), similar to previous studies [14,35,37,40]. Note that each fall direction is represented by a α–β pair henceforth (e.g., 10°–15°: $\alpha = 10°$ and $\beta = 15°$).

Boundary conditions simulating the complex loading and constraining conditions in the experimental sideways fall setting [53] were used in the present study (Fig. 2). The loading force and restraining conditions were applied through polymethyl methacrylate (PMMA) caps and an aluminum distal pot. All materials were modeled with 10-noded tetrahedral finite elements and a 2 mm element size was used for the entire proximal femur, the PMMA caps, and the boundary between the distal end of the proximal femur bone and the distal pot. The convergence analysis was conducted with four different element sizes (4 mm, 3 mm, 2 mm, and 1 mm) in the FE model (in 10°–15°) using 30 randomly selected proximal femora, five from each group. The converged solution was obtained by extrapolating the fracture loads from these element-sized FE models. Compared to the converged solution, the mean absolute percentage error in the fracture load for 4 mm, 3 mm, 2 mm, and 1 mm element-sized FE models were 5.5%, 4.7%, 2.9%, and 2.2%, respectively. Furthermore, the absolute errors in the relative difference in bone strength (Section 2.4) were 3.6%, 4.1%, 1.5%, and 1.6%, respectively. The 2 mm element size was considered acceptable, as the estimated errors remained consistently below 3%. Fracture load was estimated using a simple maximum principal strain criterion [53,54], described in detail elsewhere [31,53]. MATLAB (MathWorks, Inc., Natick, MA, USA) was used to estimate the fracture load. MFS (minimum fall strength) was defined as the lowest fracture load among the 12 different fall configurations in each proximal femur [35,36,40].

2.4. Statistical analysis

Statistical analyses were performed using SPSS 25.0 (IBM Corp., Armonk NY, USA). Mean and standard deviation (SD) of participants' background characteristics, fall direction-wise fracture loads, and MFSs were given as descriptive statistics. Prior to following statistical analyses, logarithmic transformation of the fall direction-wise fracture load and MFS were performed to control for the skewness of the data, and the normality of the transformed data was confirmed by the Shapiro-Wilk test.

The primary objective of the present study was addressed in three different statistical analyses. First, a two-way repeated measures analysis of variance (ANOVA) was performed to evaluate the association of fall angles α and β with fracture loads within each group. A Sidak correction was used to control for multiple comparisons in this analysis. Second, a split-plot ANOVA was performed to evaluate whether the potential associations and interactions of α and β with the fracture loads differed between the groups. Third, both one-way ANOVA and analysis of covariance (ANCOVA) using BW or LM as a covariate were performed to estimate the differences in the fracture loads between each exercise loading group and the control group in each fall direction. Covariates were selected through the following process. Pearson correlation analyses showed that the height, BW, and LM had significant ($p < 0.05$) low-to-moderate correlations ($r = 0.29$, 0.33 and 0.50, respectively) with

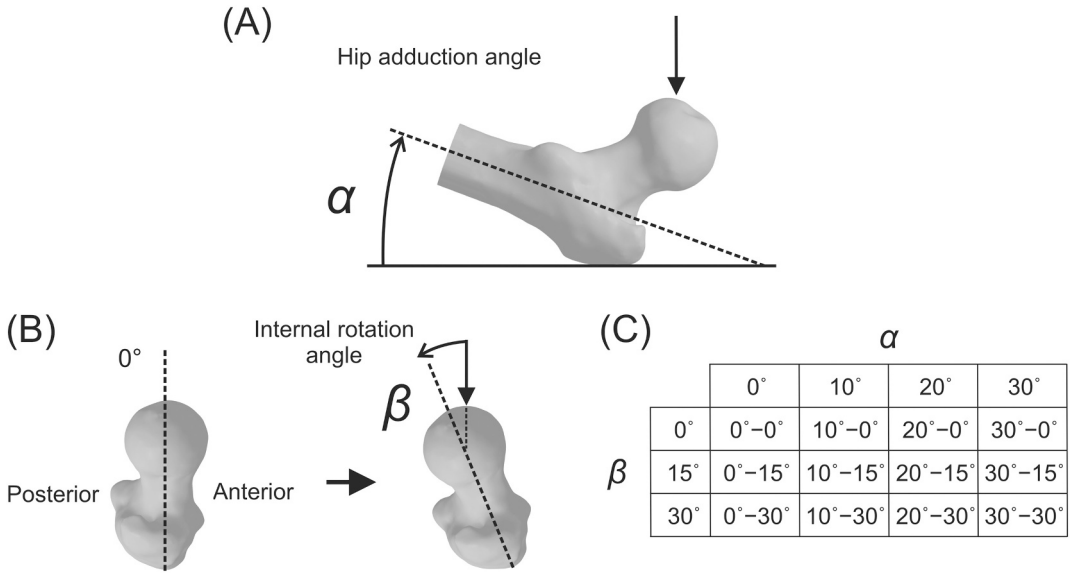

β \ α	0°	10°	20°	30°
0°	0°–0°	10°–0°	20°–0°	30°–0°
15°	0°–15°	10°–15°	20°–15°	30°–15°
30°	0°–30°	10°–30°	20°–30°	30°–30°

Fig. 1. Multiple sideways fall configuration. An angle α denotes the hip adduction angle or the angle between the femoral shaft and the ground (A) while the angle β denotes the internal rotation angle of femoral neck (B). This angle α was rotated in steps from 0°, 10°, 20°, to 30° while the angle β was increased in steps from 0°, 15°, and 30°. A total of 12 different fall directions were simulated by combining four α angles and three β angles, and each direction is represented by a $\alpha - \beta$ pair (C).

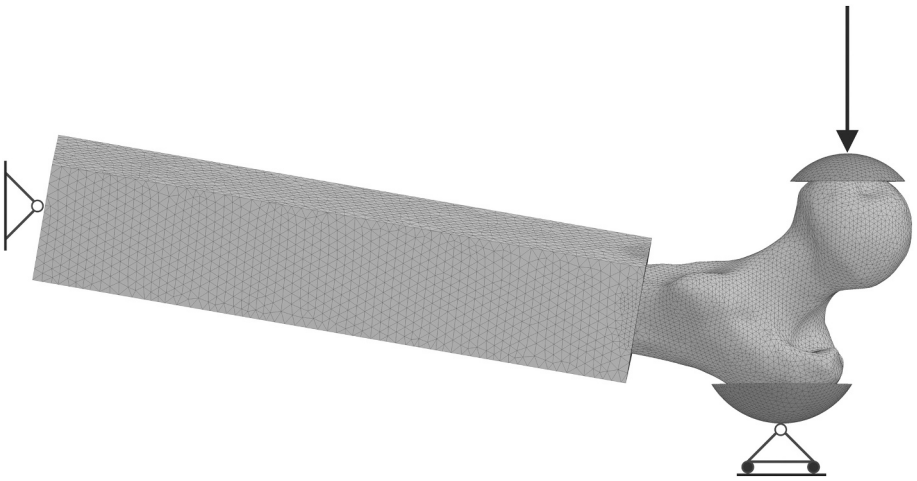

Fig. 2. Boundary conditions of the FE model. The loading force was applied to the whole upper face of the head-protecting PMMA cap at defined angles while the restraining boundary condition was applied to the trochanter PMMA cap, prohibiting the movement in the direction of the force [53]. A 200 mm long aluminum pot was installed at 15–20 mm below the most projected part of the lesser trochanter of each proximal femur. A hinge-type restraining boundary condition was assigned to the distal face of the aluminum pot, allowing nodes at the hinge-axis to freely rotate in the quasi-frontal plane whereas all other degrees of freedom were constrained. Young's modulus of 70 GPa and 2 GPa were applied to aluminum pot and PMMA cup respectively [53]. All materials were modeled with a 10-noded tetrahedral finite element and 2 mm element size was used for the entire proximal femur, the PMMA caps, and the boundary between the distal end of the proximal femur bone and the distal pot. The rest of the distal pot was modeled with 4 mm-sized element. Each proximal femur model, on average, had 194,000 elements and 292,000 nodes.

fracture loads, but the age did not ($r = 0.02$, $p = 0.76$). Also, the assumption of homogeneity of regression slopes was violated for age and height. Given these, BW and LM were used separately as the covariate in ANCOVA. Percentage differences in the fracture load between each exercise loading group and the control group (relative differences in bone strength) were calculated for each fall configuration by taking anti-log of unadjusted, BW-adjusted, and LM-adjusted mean fracture loads.

For the secondary objective, the differences in the MFS between each exercise loading group and the control group were also estimated by the ANOVA and ANCOVA using BW or LM as the covariate. The percentage difference was calculated similarly. A p-value of less than 0.05 was considered statistically significant.

3. Results

3.1. Descriptive data of participants

Group-wise descriptive data of age, height, weight, fat-%, lean body mass, and training histories characterized by the duration of competing career, the number of weekly training sessions, and weekly sport-specific training hours are presented in Table 1. The weekly mean training volume was at least three times higher among the athletic groups compared to the control group.

3.2. Fracture load

3.2.1. General trend and effect of fall angles

Group-wise unadjusted mean (SD) fracture loads in each fall direction are presented in Table 2. In every group, the highest mean fracture loads were observed in the 0°–0° direction. The lowest mean values were observed in the 30°–30° direction in all groups except for the H-I and control groups where the lowest values were in the 30°–15° direction. In general, when the angle α between the femoral shaft and the ground increased from 0° to 30°, the mean fracture loads decreased by 32–35%, 22–26%, and 12–15% at $\beta = 0°$, 15°, and 30°, respectively among the six groups investigated. Similarly, when the hip internal rotation angle β increased from 0° to 30°, the mean fracture loads decreased by 22–27%, 12–18%, 6–11%, and 1–7% at $\alpha = 0°$, 10°, 20°, and 30°, respectively. When both angles shifted from 0°–0° to 30°–30° fall direction, the mean fracture loads decreased by 34–36%.

The above consistent reductions in the mean fracture load were indicated by the two-way repeated-measures ANOVA which showed significant interactions of α and β ($p < 0.001$) with fracture loads within each group. However, according to the split-plot ANOVA, the interaction of α and/or β with the fracture loads did not differ statistically between the groups ($p = 0.601$, 0.507, and 0.151 for terms α**group*, β**group*, and α*β**group*, respectively). However, the total mean fracture loads calculated by averaging the fracture loads from all 12 fall configurations indicated a significant between-group difference ($p = 0.033$). Compared to the control group (mean ± SD: 2867 ± 500 N), the total mean fracture loads of H-I (3259 ± 388 N, $p = 0.007$), O-I (3146 ± 389 N, $p = 0.046$), and R-I (3257 ± 485 N, $p = 0.018$) were significantly different while those of H-M (2971 ± 542 N, $p = 0.541$) and R-NI (3054 ± 471 N, $p = 0.220$) were not.

3.2.2. Fall direction-wise fracture load

The percentage differences in unadjusted and BW-adjusted mean fracture loads between each exercise loading group and the control group in each fall direction are shown in Fig. 3. Both unadjusted and BW-adjusted fracture loads in the H-I and R-I groups were significantly ($p < 0.05$) higher in all 12 fall directions compared to the control group, except for the near-significant difference for the unadjusted fracture

Table 1
Descriptive group characteristics.

Group	N	Age (years)	Height (cm)	Weight (kg)	Fat-%	Lean body mass (kg)	Competing career (years)	Training sessions/week	Sport-specific training hours/week
H-I	19	22.3 (4.1)	174 (6)	60.2 (5.4)	20.0 (3.9)	45.9 (3.1)	10.1 (3.4)	6.7 (1.4)	11.5 (2.3)
O-I	19	25.3 (6.7)	165 (8)	60.8 (8.3)	25.1 (5.9)	43.3 (4.2)	9.6 (4.8)	5.7 (1.4)	9.3 (2.7)
H-M	17	27.5 (6.3)	158 (3)	63.3 (13.2)	27.9 (7.4)	43.2 (5.9)	8.0 (4.7)	5.8 (2.0)	9.1 (2.7)
R-I	18	28.9 (5.6)	168 (5)	53.7 (3.4)	14.2 (3.6)	44.1 (3.1)	12.4 (6.7)	8.7 (2.1)	10.9 (3.4)
R-NI	18	19.7 (2.4)	173 (5)	65.1 (5.6)	25.1 (5.5)	46.7 (3.5)	9.1 (2.6)	11.4 (2.0)	19.9 (4.5)
Control	20	23.7 (3.8)	164 (5)	60.0 (7.4)	31.7 (5.8)	39.0 (4.2)	–	2.8 (1.0)	2.8 (0.9)

Mean and (SD).

Table 2
Unadjusted mean (SD) estimated fracture load (in N) and p values from ANOVA and ANCOVA (only BW-adjusted). A p value in each cell is the one from ANOVA (unadjusted) while a p^* is the one from ANCOVA (BW-adjusted). The p values from ANCOVA with LM as the covariate are not included in this table since they are all nonsignificant ($p > 0.15$).

H-I	$\alpha = 0°$	$\alpha = 10°$	$\alpha = 20°$	$\alpha = 30°$
$\beta = 0°$	**4311 (565)**	**3551 (423)**	**3141 (352)**	**2951 (332)**
	$p = 0.044$, $p^* = 0.031$	**$p = 0.018$, $p^* = 0.009$**	**$p = 0.008$, $p^* = 0.003$**	**$p = 0.004$, $p^* = 0.001$**
$\beta = 15°$	**3803 (512)**	**3268 (410)**	**2995 (374)**	**2826 (357)**
	$p = 0.018$, $p^* = 0.010$	**$p = 0.013$, $p^* = 0.007$**	**$p = 0.009$, $p^* = 0.005$**	**$p = 0.007$, $p^* = 0.004$**
$\beta = 30°$	**3356 (415)**	**3112 (424)**	**2944 (425)**	**2855 (420)**
	$p = 0.003$, $p^* = 0.002$	**$p = 0.004$, $p^* = 0.002$**	**$p = 0.009$, $p^* = 0.006$**	**$p = 0.012$, $p^* = 0.009$**
O-I	$\alpha = 0°$	$\alpha = 10°$	$\alpha = 20°$	$\alpha = 30°$
$\beta = 0°$	4253 (612)	**3507 (481)**	3017 (389)	2816 (388)
	$p = 0.09$, $p^* = 0.10$	**$p = 0.045$, $p^* = 0.047$**	$p = 0.074$, $p^* = 0.076$	$p = 0.07$, $p^* = 0.071$
$\beta = 15°$	3673 (437)	**3189 (440)**	**2907 (401)**	**2747 (382)**
	$p = 0.065$, $p^* = 0.068$	**$p = 0.048$**, $p^* = 0.051$	**$p = 0.043$, $p^* = 0.046$**	**$p = 0.036$, $p^* = 0.039$**
$\beta = 30°$	3156 (396)	**2947 (335)**	2809 (338)	2734 (330)
	$p = 0.079$, $p^* = 0.083$	**$p = 0.042$, $p^* = 0.044$**	$p = 0.051$, $p^* = 0.055$	$p = 0.0504$, $p^* = 0.054$
H-M	$\alpha = 0°$	$\alpha = 10°$	$\alpha = 20°$	$\alpha = 30°$
$\beta = 0°$	4029 (838)	3351 (633)	2950 (508)	2724 (439)
	$p = 0.663$, $p^* = 0.973$	$p = 0.401$, $p^* = 0.701$	$p = 0.297$, $p^* = 0.540$	$p = 0.326$, $p^* = 0.599$
$\beta = 15°$	3379 (660)	2952 (584)	2760 (534)	2628 (475)
	$p = 0.907$, $p^* = 0.551$	$p = 0.684$, $p^* = 0.838$	$p = 0.414$, $p^* = 0.765$	$p = 0.308$, $p^* = 0.590$
$\beta = 30°$	2937 (518)	2743 (520)	2631 (542)	2568 (522)
	$p = 0.839$, $p^* = 0.637$	$p = 0.711$, $p^* = 0.752$	$p = 0.671$, $p^* = 0.791$	$p = 0.614$, $p^* = 0.877$
R-I	$\alpha = 0°$	$\alpha = 10°$	$\alpha = 20°$	$\alpha = 30°$
$\beta = 0°$	**4387 (783)**	**3624 (643)**	**3190 (548)**	**3004 (482)**
	$p = 0.053$, **$p^* = 0.002$**	**$p = 0.025$, $p^* < 0.001$**	**$p = 0.015$, $p^* < 0.001$**	**$p = 0.006$, $p^* < 0.001$**
$\beta = 15°$	**3780 (607)**	**3258 (524)**	**2986 (471)**	**2860 (451)**
	$p = 0.048$, $p^* = 0.001$	**$p = 0.034$, $p^* < 0.001$**	**$p = 0.023$, $p^* < 0.001$**	**$p = 0.01$, $p^* < 0.001$**
$\beta = 30°$	**3277 (425)**	**3014 (392)**	**2894 (395)**	**2807 (388)**
	$p = 0.021$, $p^* < 0.001$	**$p = 0.024$, $p^* < 0.001$**	**$p = 0.022$, $p^* < 0.001$**	**$p = 0.026$, $p^* < 0.001$**
R-NI	$\alpha = 0°$	$\alpha = 10°$	$\alpha = 20°$	$\alpha = 30°$
$\beta = 0°$	4133 (630)	3390 (511)	2936 (451)	2699 (393)
	$p = 0.267$, $p^* = 0.844$	$p = 0.205$, $p^* = 0.896$	$p = 0.270$, $p^* = 0.931$	$p = 0.356$, $p^* = 0.743$
$\beta = 15°$	3610 (634)	3111 (519)	2826 (443)	2682 (417)
	$p = 0.217$, $p^* = 0.795$	$p = 0.165$, $p^* = 0.716$	$p = 0.160$, $p^* = 0.749$	$p = 0.125$, $p^* = 0.699$
$\beta = 30°$	3033 (500)	2835 (474)	2728 (464)	2669 (463)
	$p = 0.422$, $p^* = 0.935$	$p = 0.316$, $p^* = 0.955$	$p = 0.254$, $p^* = 0.871$	$p = 0.218$, $p^* = 0.813$
Control	$\alpha = 0°$	$\alpha = 10°$	$\alpha = 20°$	$\alpha = 30°$
$\beta = 0°$	3902 (709)	3176 (544)	2776 (470)	2583 (427)
$\beta = 15°$	3360 (644)	2877 (564)	2622 (502)	2474 (444)
$\beta = 30°$	2905 (494)	2683 (465)	2558 (477)	2487 (485)

Statistically significant p values ($p < 0.05$) based on ANOVA and ANCOVA are shown in bold.

load in the R-I group in the 0°–0° direction ($p = 0.053$) (Table 2). The unadjusted and BW-adjusted percentage differences in the H-I group ranged from 11% to 17% compared to the control group (Fig. 3). Similarly, the unadjusted and BW-adjusted differences in the R-I group ranged from 13% to 16% and 22 to 28%, respectively (Fig. 3).

The unadjusted and BW-adjusted fracture loads in the O-I group were significantly higher in five fall directions (10°–0°, 10°–15°, 10°–30°, 20°–15°, and 30°–15°), except there was a near-significant ($p = 0.051$) difference for the BW-adjusted fracture load in the 10°–15° direction, compared to the controls (Table 2). In these directions, the unadjusted and BW-adjusted percentage differences in the O-I group ranged from 11% to 12% and 10% to 11%, respectively (Fig. 3). In the rest of the fall directions in the O-I group, there were trends ($p \leq 0.1$) for 9% to 11% higher unadjusted and BW-adjusted fracture load (Table 2 and Fig. 3).

The mean fracture loads in the H-M and R-NI groups did not differ significantly from the controls in any fall direction (Table 2). Compared to the control group, the unadjusted and BW-adjusted percentage differences in the H-M group ranged from 1% to 6% and − 3% to 3% throughout the 12 fall directions, respectively (Fig. 3). Those in the R-NI group ranged from 5% to 9% and − 2 to 2%, respectively (Fig. 3).

In contrast, once adjusted for LM, none of the exercise loading groups had significantly higher fracture loads in any fall direction compared to the control group ($p > 0.05$). Respective LM-adjusted percentage differences in each exercise loading group ranged in the 12 fall configuration as follows: H-I, from 0% to 5%, $p > 0.42$; O-I, from 2% to 6%, $p > 0.35$; H-M, from −8% to −1%, $p > 0.16$; R-I, from 0% to 4%, $p > 0.53$; and R-NI, from −10% to −6%, $p > 0.15$. Exact values of the unadjusted, BW-adjusted, and LM-adjusted percentage differences with 95% CI in all exercise loading groups compared to controls are given in the Supplementary data (Table A-1).

3.2.3. Minimum fall strength (MFS)

The occurrence of MFS in each fall configuration is shown in Table 3. The MFSs occurred only when either or both of the fall angles α and β were the greatest: 1 in the 10°–30°, 13 in the 20°–30°, 23 in the 30°–0°, 34 in the 30°–15°, 40 cases in the 30°–30°.

Group-wise unadjusted mean (SD) MFSs and the percentage differences in the unadjusted, BW-adjusted, and LM-adjusted mean MFSs between each exercise loading group and the control group are presented in Table 4. Compared to the control group, the unadjusted MFSs in the H-I, O-I, and R-I groups were significantly ($p < 0.05$) 15%, 11%, and 14% higher while their BW-adjusted MFSs were significantly 15%, 11%, and 26% higher, respectively (Table 4). The unadjusted and BW-adjusted MFSs in the H-M and R-NI groups did not significantly differ

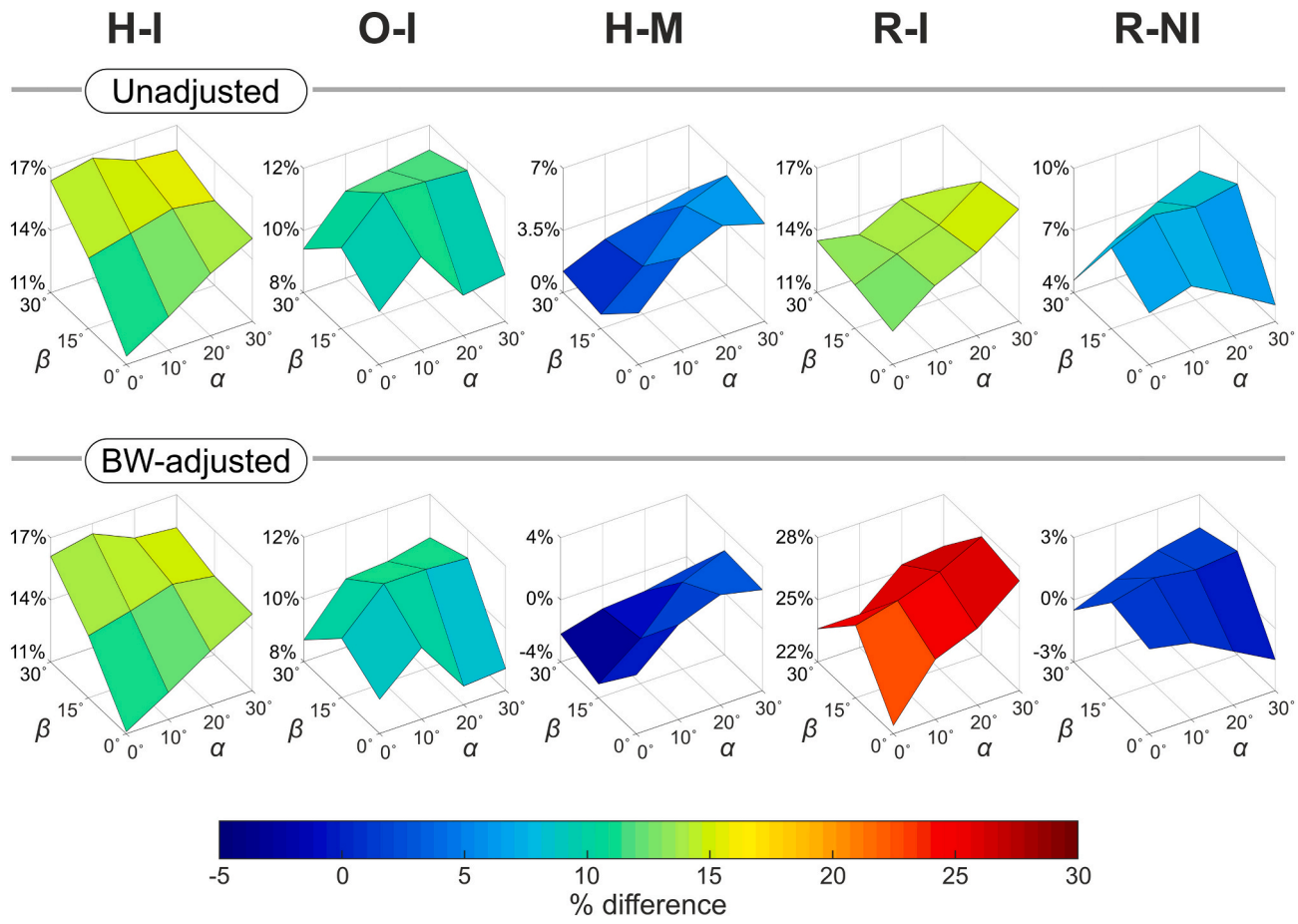

Fig. 3. Unadjusted and BW-adjusted mean percentage (%) differences in the fracture loads of exercise loading groups compared to the control group. Vertical axis in each surface plot shows % difference.

Table 3
The number of MFS observed in each falling configuration. The column for α = 0° is omitted since there was no MFSs observed in that direction.

	$\alpha = 10^\circ$		$\alpha = 20^\circ$		$\alpha = 30^\circ$	
$\beta = 0^\circ$					H-I	5
					O-I	6
					H-M	2
					R-I	1
					R-NI	6
					Control	3
					Total	**23**
$\beta = 15^\circ$					H-I	5
					O-I	5
					H-M	4
					R-I	8
					R-NI	3
					Control	9
					Total	**34**
$\beta = 30^\circ$			H-I	2	H-I	7
			O-I	2	O-I	6
			H-M	4	H-M	7
	R-I	1	R-I	2	R-I	6
			R-NI	2	R-NI	7
			Control	1	Control	7
	Total	**1**	**Total**	**13**	**Total**	**40**

from the control group. Lastly, none of the exercise loading groups had significantly different LM-adjusted MFS compared to the controls (Table 4).

4. Discussion

In the present study, we elaborated whether the higher bone strength in athletes attributed to specific exercise loading history persisted regardless of the fall direction. This analysis was performed by simulating proximal femur FE models of 91 female athletes, representing several distinct exercise loading types, and their 20 controls in multiple fall directions and estimated the corresponding fracture loads. The fall directions were associated with the fracture loads in all groups. Overall, the fracture loads decreased by 12–35% as the tilt angle (α) of the femoral shaft increased from 0° to 30°, 1–27% as the hip internal rotation angle (β) increased from 0° to 30°, and 34–36% as both angles increased from 0° to 30°. These trends are in line with previous experimental [32] and FE modeling studies of the multiple fall configurations [33–36]. However, it is noted that the two FE studies [35,36] reported slightly different decreases in the fracture load due to changes in α or β alone and both of them; respective decreases were 4–12%, 14–20%, and 24% [35], and 33–36%, 7–15%, and 38% [36]. The exact reasons behind these discrepancies remain unknown. However, we speculate that they were likely due to young and athletic participants of the present study and methodological differences in the FE models (e.g., the use of homogeneous material property assignment and different distal

Table 4
Minimum fall strength (MFS) – unadjusted mean (SD) MFS (in N) and percentage differences in unadjusted, BW-, or LM-adjusted mean MFSs between each exercise group and the control group with 95CI.

Group	MFS mean (SD)	Unadjusted	*p*	BW-adjusted	*p*	LM-adjusted	*p*
		% diff		% diff		%diff	
H-I	**2761 (366)**	**14.9 (3.4 to 27.6)**	**0.011**	**14.5 (3.9 to 26.2)**	**0.007**	3.1 (−10.0 to 18.2)	0.652
O-I	**2674 (346)**	**11.3 (0.2 to 23.5)**	**0.046**	**10.6 (0.1 to 22.1)**	**0.048**	4.3 (−6.5 to 16.4)	0.440
H-M	2527 (465)	4.4 (−7.7 to 18.1)	0.484	0.6 (−8.9 to 11.1)	0.900	−3.9 (−14.2 to 7.7)	0.486
R-I	**2752 (371)**	**14.4 (2.5 to 27.6)**	**0.018**	**25.9 (13.2 to 40.1)**	**<0.001**	1.4 (−9.6 to 13.8)	0.804
R-NI	2576 (381)	7.0 (−4.3 to 19.6)	0.229	0.7 (−9.6 to 12.3)	0.891	−7.3 (−19.8 to 7.2)	0.298
Control	2425 (452)	–	–	–	–	–	–

Statistically significant *p* values ($p < 0.05$) based on ANOVA and ANCOVA are shown in bold.

constraining conditions). Altogether, these findings suggest that hip fracture risk increases if the fall impact is imposed on a more superior aspect (reflected by a greater α angle) and/or more posterolateral aspect (reflected by a greater β angle) than the lateral aspect (e.g., 0°–0° condition) of the greater trochanter. In fact, a recent cohort study of video-captured falls of over 600 elderly persons demonstrated that 77% (23 out of 30 cases) of the fall-induced hip fractures were sustained when the impact was imposed on the posterolateral aspect while 13% of hip fractures occurred when the impact was imposed on the lateral aspect [55].

A particularly important finding in the present study, based on the fall direction-wise fracture loads, was that the mean fracture loads in the H-I and R-I groups were significantly higher (11–17% and 22–28%, respectively) compared to the control group regardless of the fall direction. In contrast, the mean fracture loads in the O-I group were significantly higher (10–11%) in fewer fall directions. These results suggest that the higher bone strength against the hip fracture risk associated with H-I and the R-I exercise loading types seems robust regardless of fall direction whereas the benefit attributed to O-I exercise loading appears more modest and specific to the fall direction.

The aforementioned benefits in the H-I, O-I, and R-I groups were further confirmed by the significantly higher MFSs (15%, 11%, and 26%, respectively) compared to the control group. Importantly, Falcinelli et al. [35] and Qasim et al. [40] found that MFS from the multiple fall conditions can predict the hip fracture risk slightly more accurately than a single direction-load (e.g., 10°–15°), aBMD (femoral neck, trochanteric, and total femur), and FRAX: areas under the curve (AUC) in the receiver operating characteristics for these variables were 0.79–0.88, 0.77, 0.73–0.79, and 0.69, respectively. This highlights the importance of not only simulating multiple fall directions but also analyzing the minimum fall strength among them. It is important to note that the group-wise mean MFSs ranged from 2425 N to 2761 N in the present study (Table 4) which were quite comparable to those (2060–2729 N) observed in another multiple fall FE study by Altai et al. [36] and the two above-mentioned FE studies [35,40].

The analysis of the fall direction-wise fracture loads suggest that the weakest fall orientation of the proximal femur takes place when both of the α and β angles reach their maximum (30°–30°). The highest 36% occurrence of MFSs (40 out 111 cases, Table 3) corresponded to this orientation similar to previous studies employing the multiple fall conditions [35,40]. However, it is noted that the occurrence of MFS in the other studies was more widespread among the fall directions including even the lateral fall direction (0°–0°) [35,40], whereas the present occurrence of MFSs was more concentrated on the greatest values of either or both α and β. We hypothesize again that this discrepancy can be attributed to the differences in characteristics of participants and methodologies between studies.

One interesting observation in the present study is that the benefits observed in unadjusted and BW-adjusted higher fracture loads among the specific exercise loading groups disappeared once controlled for LM. According to bone's functional adaptation [2,3], the bone adapts to the prevalent mechanical environment, which does not exclude the contribution from the fat mass. It is the body weight that largely determines the magnitude of mechanical loading. The mechanical environment of bone comprises the gravitational ground reaction forces both in static (e.g., lying, sitting, and standing) and dynamic situations (e.g., daily physical activities such as walking, stair ambulation and sport-specific exercises such as running and jumping) as well as the internal muscle contraction forces [56]. LM can be used as a proxy for muscle mass and also muscle forces. However, the muscle mass does not necessarily equate with the actual maximal muscle forces employed in specific dynamic performances. High muscle force largely results from vigorous, long-term physical training that improves specific muscle performance via increased muscle mass and cross-sectional area, and/or enhanced neuromuscular networks [57]. Nonetheless, controlling the bone strength for muscle force (or its proxy LM) may eliminate the anabolic effect of exercise training on the bone that was the focus of the present study. The present study demonstrated this while pinpointing the importance of selecting the reasonable covariate for the research questions. In this respect, BW is a reasonable covariate as it takes into account both the person's body size and the loading caused by habitual weight-bearing physical activities and related ground reaction forces [56].

The present beneficial observations in the H-I, O-I, and R-I groups are likely attributed to exercise-induced structural adaptation in the cortical bone. Based on our previous study of the same proximal femur data [29], the femoral neck in the H-I group has ~10% thicker superior cortex, ~20% thicker anterior and posterior cortex, and notably 60% thicker weight-bearing inferior cortex compared to the controls while the O-I group has consistently 15–20% thicker cortical bone around the femoral neck. Compared to O-I exercise loading, a remarkable adaptation inherent to H-I exercise loading is ~60% thicker cortex in the weight-bearing inferior femoral neck compared to the controls [29]. Finding an effective exercise to load and strengthen the fracture-prone superolateral femoral neck has been the primary focus in previous studies [29,58–63]. However, should this be difficult, the importance of thickening the inferior cortex ought not to be underestimated. From an engineering perspective, thickening the inferior cortex would lead to an inferior shift of the neutral axis of the femoral neck in bending. Such a shift increases the bone cross-sectional area above the axis where compressive force is applied in the sideways fall situation, and thus decreases the magnitude of load (stress or strain) at the superior femoral neck. This was also suggested in a recent proximal femur FE modeling study of young adult male athletes by Warden et al. [58]. However, it is also noted that the neutral axis is also a function of the loading direction. Besides, the contribution of even a small amount of bone to fracture

prevention is greater if the bone accrual occurs at the structurally weakest location in terms of a typical fall direction. Elderly people typically display modest osteogenic responses to exercise training, and then adding even a small amount of bone at the critical location of the proximal femur may reduce the risk of hip fracture. In fact, in a 12-month exercise RCT of older males aged 70 years, Allison et al. [60] reported that daily multidirectional moderate impact hopping exercise, generating impact magnitudes of about 3 BW, resulted in regional bone accrual also at the fracture-prone superolateral cortex. Nonetheless, whether such a regional adaptation at the femoral neck would contribute to the fracture prevention remains speculative and calls for a further study examining, e.g., whether thickening inferior cortex can compensate for superior cortex thinning and its effect on the fracture load.

The higher femoral strength attributed to H-I or moderate impact exercise loadings has also been reported in recent studies of young male and female athletes by Warden et al. and Fuchs et al. [58,63]. Warden et al. [58] reported that the FE-estimated bone strength in the male jumpers, representing H-I exercise loading, was significantly higher in the sideways fall situation compared to the matched controls, similar to the present results of female athletes. Fuchs et al. [63] also demonstrated that female softball pitchers exhibited 11% dominant-to-nondominant leg side differences in the FE-estimated yield strength in the sideways fall. The softball pitching imposes an asymmetric loading such that the dominant leg, the contralateral side to their throwing arm, experiences more impact-generating landing than the non-dominant leg. This finding further confirms the benefit of impact loading on the proximal femur strength.

In contrast to the H-I and O-I groups, the R-I group did not show such regional cortical thickening of the femoral neck [29]. This indicates that the observed substantial benefit in the bone strength attributed to R-I exercise loading reflects other mechanical factors than the cortical thickness. The femoral neck cross-section in the R-I group appeared more circular [64], which provides a mechanically more robust structure in all directions compared to an oval-shaped bone. A recent study identified the femoral neck roundness as an important geometric factor among other geometrical parameters that determines its strength against fall-induced fracture [65]. Similarly, 1.3–1.5 times lower fall-induced stress was estimated in a more circular femoral neck cross-section of medieval people compared to the oval-shaped femoral neck of present-day, habitually more sedentary people [66]. The present BW-adjusted 22–28% higher fracture load in the R-I group complies closely with this estimation. However, these considerations are speculative and the apparent benefits in the proximal femur strength in the R-I group warrant further investigation.

No benefit in bone strength was observed in the H-M and R-NI groups in any fall direction. Likewise, their MFSs were not any higher than the controls. These findings most likely reflect the lack of beneficial structural adaptations in the proximal femora of these groups [24,29].

Exploring the loading characteristics of the five distinct exercise loading types in the present study may help identify essential components that underlie loading-specific beneficial adaptations in the proximal femur. Peak ground reaction forces (GRF expressed in BW) and estimated maximum loading rates (BW s^{-1}) are 12–20 BW and 400–480 BW s^{-1} for H-I [67,68]; 2.5–3.5 BW and 20–180 BW s^{-1} for O-I [59,69–71]; and 2–2.5 BW and 60–150 BW s^{-1} for R-I loadings [72–74]. Despite slightly lower GRFs and loading rates in O-I and R-I exercise loading compared to H-I exercise loading, the O-I and R-I exercises naturally have higher loading frequencies. A large number of repetitive movements and high muscle activity are also involved in swimming. However, the magnitude of mechanical loads is substantially lower in water due to its buoyancy, making it an aquatic hypo-gravitational environment. Some impact in swimming may occur during the push-off phase of turning against the pool wall, but its reaction force and loading rate are essentially smaller (<1.5 BW, and <10 BW s^{-1} respectively) [75,76]. Despite the extreme weights lifted, the peak GRF in the H-M exercise (e.g. a squat and deadlift) is comparable (2–3 times BW) [77] to those in the O-I and R-I exercises. Besides, due to the nature of H-M exercises (inherent slow movement and the low number of repetitions), the loading rate (5–6 BW s^{-1}) as well as the loading frequency remain marginal compared to the impact exercises [77]. Overall, the moderate-to-high GRF alone may not be sufficient but it needs to be applied at a high loading rate or frequency to trigger the beneficial structural adaptations within the cortical bone of the proximal femur. These considerations are essentially in line with observations from previous animal experimental studies [3,9].

Information on exercise-specific GRFs and loading rates may not be sufficient to characterize effective exercises since they convey information about loading only at the ground level, but do not necessarily tell how much loading is actually transferred to the hip joint and proximal femur. Recent musculoskeletal modeling studies with the FE analyses have evaluated hip contact force (HCF) and femoral neck strain during various movements [61,62,78,79]. Compared to the HCF (4–5 BW) in walking at 4 km/h, unilateral vertical hopping and running at 6–12 km/h induced substantially higher HCFs: 7.5 BW and 6–10 BW, respectively [62,78]. In contrast, hip resistance training (abduction, adduction, flexion, and extension exercises) at 40–80% of 1 repetition maximum (RM) induced similar or even smaller HCFs than that in walking [62]. These musculoskeletal modeling studies provide estimates of joint reaction and muscle forces. However, caution is needed when interpreting these results mainly because of two reasons. First, calculations in the (inverse) kinematic analysis may amplify the noise present in the measured data and result in substantial errors in the estimated joint forces, especially in highly dynamic vigorous movements and sports performances involving maximum efforts and rapid accelerations or decelerations. Second, the estimation of muscle forces is mostly based on the optimization using energy minimization norms which most likely does not reflect the extreme performances inherent in sports. In fact, estimated muscle forces have not been validated [62].

According to classic Frost's mechanostat theory [2] and bone remodeling theory by Huiskes et al. [80,81], the osteogenic adaptive bone response is triggered if the strain magnitude and/or strain energy exceeds the homeostatic threshold around 1500 με or by 75% respectively. Pellikaan et al. [62] showed that, compared to walking at 4 km/h, unilateral vertical hopping and running at 7–9 km/h induced significantly higher compressive and tensile strains at both the inferior and superior femoral neck, exceeding the homeostatic threshold. It is noteworthy that the unilateral vertical hopping induced up to 7 times higher strain at the inferior femoral neck than walking. This may further explain the aforementioned ~60% thicker inferior femoral neck cortical bone in the H-I group [29]. Martelli et al. [79] demonstrated that unilateral long jump and bilateral vertical jump can induce considerably high strain energy at the femoral neck exceeding homeostatic value by about 500% and 200%, respectively. However, it is noted that in these studies [62,79] dynamic loading activities were discretized into several time-instances, at each of which these estimates were obtained by static FE models. Therefore, future studies should consider dynamic FE models to include the relevant dynamic bone behavior such as strain-rate dependent viscoelasticity and a potential contribution of pore pressure [82,83]. The unilateral vertical hopping can be considered a moderate H-I exercise and/or a part of the O-I exercise excluding the multidirectional components. Thus, these high HCFs, and femoral neck strain and energy induced by the jumping, hopping, and running exercises further support the effectiveness of impact exercises in triggering osteogenic adaptation within the proximal femur.

Multidirectional O-I exercise has not been specifically analyzed in the previous musculoskeletal FE modeling studies [61,62,78,79]. We hypothesized that the O-I exercise can cause more uniform strain distribution across the femoral neck due to repeated impacts from varying directions within a short period of time. Thus, it may promote a more symmetric osteogenic adaptation around the femoral neck cortical bone, including the vulnerable superolateral femoral neck. However, the hip

contact forces and femoral neck strains during O-I exercise may be smaller than those in H-I and R-I exercises. Loads generated by ground impacts from unusual directions may be largely dissipated by the activity of muscles that maintain the kinematic posture before reaching the hip joint. It is important to note that a recent review by Martelli et al. [84] analyzed the hip strains during different exercises assessed in musculoskeletal and FE modeling studies. They did not only confirm the anabolic osteogenic effect of moderate H-I exercises (e.g., vertical hopping) on the proximal femur including the fracture-prone superolateral region of the femoral neck but also suggested that the multidirectional O-I exercises may also confer such a beneficial effect owing to its non-habitual strain patterns within the femoral neck, supporting thus our speculation. Therefore, this calls for future musculoskeletal FE modeling studies to include the multidirectional O-I exercise. Besides, considering the importance of the loading rate, an additional analysis on such information at the hip joint from these musculoskeletal FE modeling studies [61,62,78,79] may further elucidate the mechanism of exercise-induced osteogenic adaptation.

The clinical relevance of present results should be interpreted with caution. Since our study was conducted in young adult females, the findings cannot be translated directly into the general or older population. However, the efficacy of the H-I, O-I, and R-I impact exercises in inducing beneficial adaptation in the femoral neck has been confirmed in several meta-analyses of RCTs regardless of age, including pre- and postmenopausal females [85–87]. Nonetheless, the feasibility of impact exercises for the older population should be carefully considered. Despite clear benefits on bone, the H-I exercise generating extreme ground reaction forces (12–20 times BW) is too risky not only for older people but also for sedentary persons regardless of age. In contrast, the risk of musculoskeletal injuries is likely lower for the O-I and R-I exercises due to more moderate impact magnitudes. Thus, these exercises can offer a safe and feasible option to increase or maintain the proximal femur strength. Moderate R-I exercises such as fast walking (6 km/h) and stair ambulation have been found to induce potentially osteogenic higher strain at the fracture-prone superior femoral neck compared to normal walking (4 km/h) [61,62,84]. Since these exercises are safe and require less effort than running, they can be easily implemented into habitual daily activities even in the elderly population. However, it should be noted that although a few meta-analyses of (R)CTs in postmenopausal females have reported that walking or combined jogging with walking and stair ambulation can increase the femoral neck aBMD, the observed increases have remained too small to be of clinical significance concerning the reduction of hip fractures [87,88]. The potential of these moderate R-I exercises is likely limited in preserving bone mass and mitigating age-related bone fragility. Whether these moderate R-I exercises can decrease the hip fracture risk is yet unclear and calls further investigation including the effective intensity (walking speed) and volume of these exercises to prevent hip fractures.

There are several limitations in the present study. First, the homogeneous material property assignment was used instead of density-based inhomogeneous material property assignment. The trabecular bone is a two-phased material comprising a mineralized bone tissue (solid phase), forming a highly porous three-dimensional lattice structure, and a fluid phase such as interstitial fluid and bone marrow, filling the interconnected pores. The apparent density due to the porosity is strongly related to mechanical properties of bone, including strength and modulus [89,90]. Ununiform distribution of apparent density and subsequent variation in the modulus within the proximal femur are typically implemented by inhomogeneous material property mapping technique in the previous QCT-based FE models [16,33–38,40,53,54,91,92]. However, this inhomogeneous material property assignment could not be realized in the present study due to the inherent limitation to the present MRI data. Nonetheless, the use of inhomogeneous material properties may have enhanced the model accuracy to some extent. However, considering that the present athletic groups have a higher proximal femur aBMD than their nonathlete peers [29], if the inhomogeneous material properties were applied in the present study, the between-group differences in the fracture load could have been higher. Moreover, the present controls were physically active and engaged in recreational exercise 2–3 times a week. Given this, the benefits observed in the exercise loading groups could have been higher if the comparisons were made against truly sedentary people. Although the use of QCT would have enabled us to include the inhomogeneous material property assignment through utilizing data on bone apparent density derived from the voxel-based Hounsfield unit, exposing fertile young adult females to ionizing X-ray radiation from QCT for non-diagnostic purposes would have been ethically unacceptable.

Moreover, the trabecular elastic modulus of 1500 MPa employed in the present study may have been too low for young and athletic females. Nicks et al. [93] reported that the mean femoral neck trabecular volumetric BMD among 20–29 years old females was 0.268 g/cm^3, which yields trabecular modulus of ~2600 MPa through the density-modulus relationship [53,90,94]. We have previously shown that the use of this high modulus would increase the estimated fracture loads by 10–15% [31], and thus in absolute terms, the present fracture loads were underestimated. However, the present study primarily aimed to evaluate the relative differences in the fracture load between groups. In our previous study [31], we also investigated the influence of varying cortical and trabecular moduli on relative between-group strengths and found only a negligible less than 3% effect by this variation. Therefore, the moduli adopted in the present study are conceivable to address the present research questions properly.

Another major limitation of the present study pertains to MRI-based FE models not being validated by an experimental mechanical testing. However, Rajapakse et al. [95] recently validated their proximal femur MRI-based FE models including inhomogeneous material property assignment. They achieved a strong agreement between experimental fracture loads and FE-derived ones ($r = 0.89$ for yield load; $r = 0.92$ for failure load). The main differences between our and their studies pertain to the field strength (1.5 T vs. 3.0 T) and the spatial resolution (0.9 mm × 0.9 mm × 1 mm vs. 0.3 mm × 0.3 mm × 0.3 mm) of the MRI system used. Because of a better signal-to-noise ratio, 3.0 T MRI achieves a higher spatial resolution than 1.5 T MRI, resulting in clearer and more detailed images. Phan et al. [96] have reported better performance for 3.0 T MRI in capturing the trabecular structure than the 1.5 T MRI. Based on the high-resolution pQCT data obtained from proximal femur ex vivo specimens from osteoporotic females aged from 67 to 94 years [97], Chang et al. [98] implied that it would be ideal if the resolution of imaging is comparable to the mean trabecular thickness varying site-specifically from 0.19 to 0.26 mm and the mean trabecular spacing varying from 0.67 mm to 0.98 mm. Among younger females aged from 16 to 66 years, the trabecular thickness and separation are comparable being 0.15 mm and 0.75 mm on average, respectively [99]. Obviously, the resolution of our MRI data is larger than these numbers and not able to capture the actual porous trabecular structure. Accordingly, we considered the inhomogeneous material property assignment unreasonable to our MRI-based FE-model.

Due to the lack of validation of our MRI-based FE model, caution is needed when interpreting the results. However, our results were quite similar to those studies which employed either the same failure criterion or presented the yield strength. The group-wise mean fracture loads from the 12 fall directions ranged from 2474 N to 4311 N in the present study of young adult females. These values were slightly higher than the mean values in QCT-based FE studies of old persons aged over 60 years where either only single fall direction (10°–15°) or multiple fall directions were simulated: 3099 N [53] in the 10°–15° direction; 2284–2995 N [35] and 1999–3227 N [36] in similar multiple fall configurations to the present study. A slightly lower mean fracture load (2342 N) was also reported in a recent MRI-based FE study of old persons with a mean age of 76 years [95]. As discussed earlier, the present fracture load values were underestimated for the young athletic females because of the low elastic modulus (1500 MPa) for trabecular bone. A recent QCT-based FE study of young adult male long and high jumpers,

baseball pitchers, and their age-matched controls showed mean fracture loads of 4519 N, 3190 N, and 2931 N in the fall direction of 10°–35°, respectively [58]. However, the fact that the participants were all male likely explains the higher values compared to the present study, where the respective group-wise mean values (10°–30°) were 2487–2855 N. Their recent FE study [63] similarly analyzed the proximal femur of young adult female softball pitchers and cross-country runners but the fracture loads were not reported. Furthermore, as discussed earlier, both the MFSs and the decreasing trends of fracture loads along with increasing fall angles were also comparable to those reported in QCT-based FE studies of the multiple fall configurations [35,36,40]. Considering the present fracture loads and their trends being comparable to those from previous QCT/MRI-based FE studies, we venture to claim that our MRI-based FE model is adequately valid, especially for evaluating the relative strength of proximal femur between exercise loading groups.

Besides the application of the homogeneous material property assignment, the proximal femur was modeled as the quasi-static linear isotropic FE models in the present study. It is known that the mechanical properties of the cortical and trabecular bones depend on the strain rate such that the elastic modulus and strength values rise as the strain rate is increased [89,100,101]. Thus, this strain-rate dependent mechanical behavior has been taken into account in recent FE studies [16,53,91]. Fall is a highly dynamic event and the impact velocity to the hip reaches approximately 3.0 m/s or higher [102]. A drawback of quasi-static modeling of the proximal femur in a fall situation is that it disregards important dynamic mechanical properties of bone such as viscoelasticity, viscoplasticity, inertia, and shock-propagation. Recent studies [91,92] have developed dynamic proximal femur FE models and observed strain rates from 1/s to 200/s [91] at elements in the femoral head, neck, and greater trochanter. These findings underline the importance of including the strain-rate dependency in future FE modeling studies. Furthermore, the complex microarchitecture of the trabecular bone results in anisotropic mechanical properties, which have also been implemented in proximal femur FE models utilizing high-resolution pQCT (spatial resolution <100 μm) [103,104]. These aspects were not considered in the present study and their inclusion would likely result in improved model accuracy.

Estimation of the fracture load in the fall is only one aspect of assessing the hip fracture risk. The risk is also largely influenced by the likelihood of the fall and fall dynamics [105,106]. Participant's body height and weight, as well as the fall-specific impact velocity, determine largely the impact force while the trochanteric soft tissue may attenuate the impact force and absorb energy during the impact [106]. Recent biofidelic dynamic FE models by Fleps et al. [92,107] demonstrated that, depending on the thickness of soft tissue, ~30–50% of the peak impact force and ~30% of impact energy can be absorbed by the soft tissue. Importantly, these findings highlight the beneficial results observed in the impact loading exercise groups since the exercise can decrease the hip fracture risk not only by increasing bone strength but also by improving neuromuscular performance, coordination, and balance. The latter improvements decrease the fall risk, and in case of a fall, more muscle tissue around the hip increases the absorption of the impact energy.

In conclusion, the present MRI-based FE study of 111 young adult females representing histories of distinct exercise loading patterns, based on 1332 pertinent FE models covering 12 multiple fall directions, demonstrated that the lower risk of hip fracture judged from higher estimated fracture loads in athletes engaged in high impact or repetitive impact sports is independent of the fall direction. In contrast, the lower fracture risk attributed to the odd-impact exercise remains more modest and specific to the fall direction. The analysis of the minimum fall strength spanning the multiple fall directions also indicated lower hip fracture risk in these athletes. In concordance with the literature, the present results confirmed that the most critical fall direction is the posterolateral direction. As a clinical prospect, the present results highlight the importance of impact exercises in combat against hip fracture, and therefore, even the elderly should be provided feasible and moderate impact exercises as strategies for falls and fracture prevention. Because the present participants were young adult females, for ethical reasons, it was necessary to use MRI in bone imaging instead of QCT, which led to employing homogeneous material property assignment and non-validated FE-models. However, a thorough comparison to the literature provided sufficient evidence for the validity of the present models and gave credibility to the findings. Lastly, the present results call for retrospective studies to investigate whether a specific impact exercise history in adolescence and young adulthood is specifically associated with a lower incidence of hip fractures in later life.

CRediT authorship contribution statement

Shinya Abe: Conceptualization, Methodology, Software, Validation, Formal analysis, Data Curation, Writing – original draft and review & editing, Visualization, Funding acquisition. **Reijo Kouhia:** Conceptualization, Writing – review & editing, Supervision, Funding acquisition. **Riku Nikander:** Conceptualization, Formal analysis, Investigation, Resources, Writing – review & editing, Supervision. **Nathaniel Narra:** Conceptualization, Investigation, Resources, Writing – review & editing, Funding acquisition. **Jari Hyttinen:** Conceptualization, Investigation, Writing – review & editing, Supervision, Funding acquisition. **Harri Sievänen:** Conceptualization, Validation, Formal analysis, Investigation, Resources, Writing – original draft and review & editing, Supervision, Funding acquisition.

Declaration of competing interest

All authors declare no conflict of interest.

Acknowledgements

This work was funded by Tampere University's (former Tampere University of Technology's: TUT) Graduate School and Industrial Research Fund; Pirkanmaa Regional Fund from Finnish Cultural Foundation; Päivikki and Sakari Sohlberg Foundation; the Doctoral Education Council of Computing and Electrical Engineering of TUT; and Human Spare Parts project from the Finnish Funding Agency for Technology and Innovation (TEKES).

Appendix A. Supplementary data

Supplementary data to this article can be found online at https://doi.org/10.1016/j.bone.2022.116351.

References

[1] N.H. Hart, S. Nimphius, T. Rantalainen, A. Ireland, A. Siafarikas, R.U. Newton, Mechanical basis of bone strength: influence of bone material, bone structure and muscle action, J. Musculoskelet. Neuronal Interact. 17 (2017) 114–139.
[2] H.M. Frost, Bone's mechanostat: A 2003 update, Anat Rec A Discov Mol Cell Evol Biol. 275 (2003) 1081–1101.
[3] C. Ruff, B. Holt, E. Trinkaus, Who's afraid of the big bad Wolff?: "Wolff's law" and bone functional adaptation, Am. J. Phys. Anthropol. 129 (2006) 484–498.
[4] C.M. Weaver, C.M. Gordon, K.F. Janz, H.J. Kalkwarf, J.M. Lappe, R. Lewis, M. O'Karma, T.C. Wallace, B.S. Zemel, The National Osteoporosis Foundation's position statement on peak bone mass development and lifestyle factors: a systematic review and implementation recommendations, Osteoporos. Int. 27 (2016) 1281–1386.
[5] B.A. Wallace, R.G. Cumming, Systematic review of randomized trials of the effect of exercise on bone mass in pre- and postmenopausal women, Calcif. Tissue Int. 67 (2000) 10–18.
[6] W. Kemmler, K. Engelke, S. von Stengel, Long-term exercise and bone mineral density changes in postmenopausal women-are there periods of reduced effectiveness? J. Bone Miner. Res. 31 (2016) 215–222.
[7] M. Kistler-Fischbacher, B.K. Weeks, B.R. Beck, The effect of exercise intensity on bone in postmenopausal women (part 1): a systematic review, Bone 143 (2021), 115696.

[8] R. Nikander, H. Sievänen, A. Heinonen, R.M. Daly, K. Uusi-Rasi, P. Kannus, Targeted exercise against osteoporosis: a systematic review and meta-analysis for optimising bone strength throughout life, BMC Med. 8 (2010) 47.
[9] T.M. Skerry, One mechanostat or many? Modifications of the site-specific response of bone to mechanical loading by nature and nurture, J Musculoskelet Neuronal Interact. 6 (2006) 122–127.
[10] N. Veronese, H. Kolk, S. Maggi, Epidemiology of fragility fractures and social impact, in: P. Falaschi, D. Marsh (Eds.), Orthogeriatrics Manag Older Patients with Fragility Fract, Springer, Cham, 2020, pp. 19–34.
[11] J. Parkkari, P. Kannus, M. Palvanen, A. Natri, J. Vainio, H. Aho, I. Vuori, M. Järvinen, Majority of hip fractures occur as a result of a fall and impact on the greater trochanter of the femur: a prospective controlled hip fracture study with 206 consecutive patients, Calcif. Tissue Int. 65 (1999) 183–187.
[12] C.M. Court-Brown, N.D. Clement, A.D. Duckworth, L.C. Biant, M.M. McQueen, The changing epidemiology of fall-related fractures in adults, Injury 48 (2017) 819–824.
[13] P.M. de Bakker, S.L. Manske, V. Ebacher, T.R. Oxland, P.A. Cripton, P. Guy, During sideways falls proximal femur fractures initiate in the superolateral cortex: evidence from high-speed video of simulated fractures, J. Biomech. 42 (2009) 1917–1925.
[14] L. Zani, P. Erani, L. Grassi, F. Taddei, L. Cristofolini, Strain distribution in the proximal human femur during in vitro simulated sideways fall, J. Biomech. 48 (2015) 2130–2143.
[15] L. Grassi, J. Kok, A. Gustafsson, Y. Zheng, S.P. Väänänen, J.S. Jurvelin, H. Isaksson, Elucidating failure mechanisms in human femurs during a fall to the side using bilateral digital image correlation, J. Biomech. 106 (2020), 109826.
[16] B. Helgason, S. Gilchrist, O. Ariza, J.D. Chak, G. Zheng, R.P. Widmer, S. J. Ferguson, P. Guy, P.A. Cripton, Development of a balanced experimental-computational approach to understanding the mechanics of proximal femur fractures, Med. Eng. Phys. 36 (2014) 793–799.
[17] B.C.C. Khoo, K. Brown, J.R. Lewis, E. Perilli, R.L. Prince, Ageing effects on 3-dimensional femoral neck cross-sectional asymmetry: implications for age-related bone fragility in falling, J. Clin. Densitom. 22 (2019) 153–161.
[18] K.E. Poole, P.M. Mayhew, C.M. Rose, J.K. Brown, P.J. Bearcroft, N. Loveridge, J. Reeve, Changing structure of the femoral neck across the adult female lifespan, J. Bone Miner. Res. 25 (2010) 482–491.
[19] J. Carballido-Gamio, R. Harnish, I. Saeed, T. Streeper, S. Sigurdsson, S. Amin, E. J. Atkinson, T.M. Therneau, K. Siggeirsdottir, X. Cheng, L.J. Melton III, J. H. Keyak, V. Gudnason, S. Khosla, T.B. Harris, T.F. Lang, Proximal femoral density distribution and structure in relation to age and hip fracture risk in women, J. Bone Miner. Res. 28 (2013) 537–546.
[20] F. Johannesdottir, B. Allaire, M.L. Bouxsein, Fracture prediction by computed tomography and finite element analysis: current and future perspectives, Curr. Osteoporos. Rep. 16 (2018) 411–422.
[21] Y.T. Lagerros, E. Hantikainen, K. Michaëlsson, W. Ye, H.O. Adami, R. Bellocco, Physical activity and the risk of hip fracture in the elderly: a prospective cohort study, Eur. J. Epidemiol. 32 (2017) 983–991.
[22] M.J. LaMonte, J. Wactawski-Wende, J.C. Larson, X. Mai, J.A. Robbins, M. S. LeBoff, Z. Chen, R.D. Jackson, A.Z. LaCroix, J.K. Ockene, K.M. Hovey, J. A. Cauley, WHI, Association of physical activity and fracture risk among postmenopausal women, JAMA Netw Open. 2 (2019), e1914084.
[23] P. de Souto Barreto, Y. Rolland, B. Vellas, M. Maltais, Association of Long-term Exercise Training with risk of falls, fractures, hospitalizations, and mortality in older adults: a systematic review and meta-analysis, JAMAIntern. Med. 179 (2019) 394–405.
[24] R. Nikander, H. Sievänen, A. Heinonen, P. Kannus, Femoral neck structure in adult female athletes subjected to different loading modalities, J. Bone Miner. Res. 20 (2005) 520–528.
[25] A. Heinonen, P. Oja, P. Kannus, H. Sievänen, H. Haapasalo, A. Mänttäri, I. Vuori, Bone mineral density in female athletes representing sports with different loading characteristics of the skeleton, Bone 17 (1995) 197–203.
[26] M. Bellver, L. Del Rio, E. Jovell, F. Drobnic, A. Trilla, Bone mineral density and bone mineral content among female elite athletes, Bone 127 (2019) 393–400.
[27] T.A. Scerpella, B. Bernardoni, S. Wang, P.J. Rathouz, Q. Li, J.N. Dowthwaite, Site-specific, adult bone benefits attributed to loading during youth: a preliminary longitudinal analysis, Bone 85 (2016) 148–159.
[28] A.S. Tenforde, M. Fredericson, Influence of sports participation on bone health in the young athlete: a review of the literature, PM R 3 (2011) 861–867.
[29] R. Nikander, P. Kannus, P. Dastidar, M. Hannula, L. Harrison, T. Cervinka, N. G. Narra, R. Aktour, T. Arola, H. Eskola, S. Soimakallio, A. Heinonen, J. Hyttinen, H. Sievänen, Targeted exercises against hip fragility, Osteoporos. Int. 20 (2009) 1321–1328.
[30] S. Abe, N. Narra, R. Nikander, J. Hyttinen, R. Kouhia, H. Sievänen, Exercise loading history and femoral neck strength in a sideways fall: a three-dimensional finite element modeling study, Bone 92 (2016) 9–17.
[31] S. Abe, N. Narra, R. Nikander, J. Hyttinen, R. Kouhia, H. Sievänen, Impact loading history modulates hip fracture load and location: a finite element simulation study of the proximal femur in female athletes, J. Biomech. 76 (2018) 136–143.
[32] T.P. Pinilla, K.C. Boardman, M.L. Bouxsein, E.R. Myers, W.C. Hayes, Impact direction from a fall influences the failure load of the proximal femur as much as age-related bone loss, Calcif. Tissue Int. 58 (1996) 231–235.
[33] J.H. Keyak, H.B. Skinner, J.A. Fleming, Effect of force direction on femoral fracture load for two types of loading conditions, J. Orthop. Res. 19 (2001) 539–544.
[34] M. Bessho, I. Ohnishi, T. Matsumoto, S. Ohashi, J. Matsuyama, K. Tobita, M. Kaneko, K. Nakamura, Prediction of proximal femur strength using a CT-based nonlinear finite element method: differences in predicted fracture load and site with changing load and boundary conditions, Bone 45 (2009) 226–231.
[35] C. Falcinelli, E. Schileo, L. Balistreri, F. Baruffaldi, B. Bordini, M. Viceconti, U. Albisinni, F. Ceccarelli, L. Milandri, A. Toni, F. Taddei, Multiple loading conditions analysis can improve the association between finite element bone strength estimates and proximal femur fractures: a preliminary study in elderly women, Bone 67 (2014) 71–80.
[36] Z. Altai, M. Qasim, X. Li, M. Viceconti, The effect of boundary and loading conditions on patient classification using finite element predicted risk of fracture, Clin. Biomech. 68 (2019) 137–143.
[37] L. Grassi, E. Schileo, F. Taddei, L. Zani, M. Juszczyk, L. Cristofolini, M. Viceconti, Accuracy of finite element predictions in sideways load configurations for the proximal human femur, J. Biomech. 45 (2012) 394–399.
[38] K.K. Nishiyama, M. Ito, A. Harada, S.K. Boyd, Classification of women with and without hip fracture based on quantitative computed tomography and finite element analysis, Osteoporos. Int. 25 (2014) 619–626.
[39] P. Bhattacharya, Z. Altai, M. Qasim, M. Viceconti, A multiscale model to predict current absolute risk of femoral fracture in a postmenopausal population, Biomech. Model. Mechanobiol. 18 (2019) 301–318.
[40] M. Qasim, G. Farinella, J. Zhang, X. Li, L. Yang, R. Eastell, M. Viceconti, Patient-specific finite element estimated femur strength as a predictor of the risk of hip fracture: the effect of methodological determinants, Osteoporos. Int. 27 (2016) 2815–2822.
[41] R. Nikander, H. Sievänen, K. Uusi-Rasi, A. Heinonen, P. Kannus, Loading modalities and bone structures at nonweight-bearing upper extremity and weight-bearing lower extremity: a pQCT study of adult female athletes, Bone 39 (2006) 886–894.
[42] H. Sievänen, T. Karstila, P. Apuli, P. Kannus, Magnetic resonance imaging of the femoral neck cortex, Acta Radiol. 48 (2007) 308–314.
[43] J. Carballido-Gamio, S. Bonaretti, I. Saeed, R. Harnish, R. Recker, A.J. Burghardt, J.H. Keyak, T. Harris, S. Khosla, T.F. Lang, Automatic multi-parametric quantification of the proximal femur with quantitative computed tomography, Quant Imaging Med Surg. 5 (2015) 552–568.
[44] D.D. Cody, F.J. Hou, G.W. Divine, D.P. Fyhrie, Short term in vivo precision of proximal femoral finite element modeling, Ann. Biomed. Eng. 28 (2000) 408–414.
[45] C.S. Rajapakse, A. Hotca, B.T. Newman, A. Ramme, S. Vira, E.A. Kobe, R. Miller, S. Honig, G. Chang, Patient-specific hip fracture strength assessment with microstructural MR imaging-based finite element modeling, Radiology 283 (2017) 854–861.
[46] G. Taubin, Curve and surface smoothing without shrinkage, in: Proc IEEE Int Conf Comput Vis, IEEE Computer Society, Cambridge, MA, USA, 1995, pp. 852–857.
[47] G.N. Duda, M. Heller, J. Albinger, O. Schulz, E. Schneider, L. Claes, Influence of muscle forces on femoral strain distribution, J. Biomech. 31 (1998) 841–846.
[48] M. Lengsfeld, J. Kaminsky, B. Merz, R.P. Franke, Sensitivity of femoral strain pattern analyses to resultant and muscle forces at the hip joint, Med. Eng. Phys. 18 (1996) 70–78.
[49] K. Polgár, H.S. Gill, M. Viceconti, D.W. Murray, J.J. O'Connor, Strain distribution within the human femur due to physiological and simplified loading: finite element analysis using the muscle standardized femur model, Proc. Inst. Mech. Eng. H J. Eng. Med. 217 (2003) 173–189.
[50] C. Öhman, M. Baleani, C. Pani, F. Taddei, M. Alberghini, M. Viceconti, M. Manfrini, Compressive behaviour of child and adult cortical bone, Bone 49 (2011) 769–776.
[51] A.D. Sylvester, P.A. Kramer, Young's modulus and load complexity: modeling their effects on proximal femur strain, Anat Rec (Hoboken). 301 (2018) 1189–1202.
[52] L. Cristofolini, G. Conti, M. Juszczyk, S. Cremonini, S. Van Sint Jan, M. Viceconti, Structural behaviour and strain distribution of the long bones of the human lower limbs, J. Biomech. 43 (2010) 826–835.
[53] E. Schileo, L. Balistreri, L. Grassi, L. Cristofolini, F. Taddei, To what extent can linear finite element models of human femora predict failure under stance and fall loading configurations? J. Biomech. 47 (2014) 3531–3538.
[54] E. Schileo, F. Taddei, L. Cristofolini, M. Viceconti, Subject-specific finite element models implementing a maximum principal strain criterion are able to estimate failure risk and fracture location on human femurs tested in vitro, J. Biomech. 41 (2008) 356–367.
[55] Y. Yang, V. Komisar, N. Shishov, B. Lo, A.M.B. Korall, F. Feldman, S. N. Robinovitch, The effect of fall biomechanics on risk for hip fracture in older adults: a cohort study of video-captured falls in long-term care, J. Bone Miner. Res. 35 (2020) 1914–1922.
[56] U.T. Iwaniec, R.T. Turner, Influence of body weight on bone mass, architecture and turnover, J. Endocrinol. 230 (2016) R115–R130.
[57] E.J. Jones, P.A. Bishop, A.K. Woods, J.M. Green, Cross-sectional area and muscular strength: a brief review, Sport Med. 38 (2008) 987–994.
[58] S.J. Warden, J. Carballido-Gamio, A.M. Weatherholt, J.H. Keyak, C. Yan, M. E. Kersh, T.F. Lang, R.K. Fuchs, Heterogeneous spatial and strength adaptation of the proximal femur to physical activity: a within-subject controlled cross-sectional study, J. Bone Miner. Res. 35 (2020) 681–690.
[59] C.A. Bailey, K. Brooke-Wavell, Optimum frequency of exercise for bone health: randomised controlled trial of a high-impact unilateral intervention, Bone 46 (2010) 1043–1049.
[60] S.J. Allison, K.E.S. Poole, G.M. Treece, A.H. Gee, C. Tonkin, W.J. Rennie, J. P. Folland, G.D. Summers, K. Brooke-Wavell, The influence of high-impact exercise on cortical and trabecular bone mineral content and 3D distribution

across the proximal femur in older men: a randomized controlled unilateral intervention, J. Bone Miner. Res. 30 (2015) 1709–1716.
[61] M.E. Kersh, S. Martelli, R. Zebaze, E. Seeman, M.G. Pandy, Mechanical loading of the femoral neck in human locomotion, J. Bone Miner. Res. 33 (2018) 1999–2006.
[62] P. Pellikaan, G. Giarmatzis, J. Vander Sloten, S. Verschueren, I. Jonkers, Ranking of osteogenic potential of physical exercises in postmenopausal women based on femoral neck strains, PLoS One. 13 (2018), e0195463.
[63] R.K. Fuchs, J. Carballido-Gamio, J.H. Keyak, M.E. Kersh, S.J. Warden, Physical activity induced adaptation can increase proximal femur strength under loading from a fall onto the greater trochanter, Bone 152 (2021), 116090.
[64] N. Narra, R. Nikander, J. Viik, J. Hyttinen, H. Sievänen, Femoral neck cross-sectional geometry and exercise loading, Clin. Physiol. Funct. Imaging 33 (2013) 258–266.
[65] R. Bryan, P.B. Nair, M. Taylor, Use of a statistical model of the whole femur in a large scale, multi-model study of femoral neck fracture risk, J. Biomech. 42 (2009) 2171–2176.
[66] H. Sievänen, L. Józsa, I. Pap, M. Järvinen, T.A. Järvinen, P. Kannus, T.L. Järvinen, Fragile external phenotype of modern human proximal femur in comparison with medieval bone, J. Bone Miner. Res. 22 (2007) 537–543.
[67] A. Heinonen, H. Sievänen, H. Kyröläinen, J. Perttunen, P. Kannus, Mineral mass, size, and estimated mechanical strength of triple jumpers' lower limb, Bone 29 (2001) 279–285.
[68] M.R. Ramey, K.R. Williams, Ground reaction forces in the triple jump, Int. J. Sport Biomech. 1 (1985) 233–239.
[69] N. Smith, R. Dyson, L. Janaway, Ground reaction force measures when running in soccer boots and soccer training shoes on a natural turf surface, Sport Eng. 7 (2004) 159–167.
[70] M.K. Dayakidis, K. Boudolos, Ground reaction force data in functional ankle instability during two cutting movements, Clin. Biomech. 21 (2006) 405–411.
[71] K. Ball, Loading and performance of the support leg in kicking, J. Sci. Med. Sport 16 (2013) 455–459.
[72] C.F. Munro, D.I. Miller, A.J. Fuglevand, Ground reaction forces in running: a reexamination, J. Biomech. 20 (1987) 147–155.
[73] S. Logan, I. Hunter, J.T. Hopkins, J.B. Feland, A.C. Parcell, Ground reaction force differences between running shoes, racing flats, and distance spikes in runners, J Sport Sci Med. 9 (2010) 147–153.
[74] B. Kluitenberg, S.W. Bredeweg, S. Zijlstra, W. Zijlstra, I. Buist, Comparison of vertical ground reaction forces during overground and treadmill running. A validation study, BMC Musculoskelet Disord. 13 (2012) 235.
[75] B.A. Blanksby, D.G. Gathercole, R.N. Marshall, Force plate and video analysis of the tumble turn by age-group swimmers, J. Swim. Res. 11 (1996) 40–45.
[76] A.D. Lyttle, B.A. Blanksby, B.C. Elliott, D.G. Lloyd, Investigating kinetics in the freestyle Flip turn push-off, J. Appl. Biomech. 15 (1999) 242–252.
[77] P.A. Swinton, R. Lloyd, J.W. Keogh, I. Agouris, A.D. Stewart, A biomechanical comparison of the traditional squat, powerlifting squat, and box squat, J. Strength Cond. Res. 26 (2012) 1805–1816.
[78] G. Giarmatzis, I. Jonkers, M. Wesseling, S. Van Rossom, S. Verschueren, Loading of hip measured by hip contact forces at different speeds of walking and running, J. Bone Miner. Res. 30 (2015) 1431–1440.
[79] S. Martelli, M.E. Kersh, A.G. Schache, M.G. Pandy, Strain energy in the femoral neck during exercise, J. Biomech. 47 (2014) 1784–1791.
[80] R. Huiskes, H. Weinans, H.J. Grootenboer, M. Dalstra, B. Fudala, T.J. Slooff, Adaptive bone-remodeling theory applied to prosthetic-design analysis, J. Biomech. 20 (1987) 1135–1150.
[81] J. Kerner, R. Huiskes, G.H. van Lenthe, H. Weinans, B. van Rietbergen, C.A. Engh, A.A. Amis, Correlation between pre-operative periprosthetic bone density and post-operative bone loss in THA can be explained by strain-adaptive remodelling, J. Biomech. 32 (1999) 695–703.
[82] T.P.M. Johnson, S. Socrate, M.C. Boyce, A viscoelastic, viscoplastic model of cortical bone valid at low and high strain rates, Acta Biomater. 6 (2010) 4073–4080.
[83] S. Le Pense, Y. Chen, Contribution of fluid in bone extravascular matrix to strain-rate dependent stiffening of bone tissue - a poroelastic study, J. Mech. Behav. Biomed. Mater. 65 (2017) 90–101.
[84] S. Martelli, B. Beck, D. Saxby, D. Lloyd, P. Pivonka, M. Taylor, Modelling human locomotion to inform exercise prescription for osteoporosis, Curr Osteoporos Rep. 18 (2020) 301–311.
[85] R. Zhao, M. Zhao, Z. Xu, The effects of differing resistance training modes on the preservation of bone mineral density in postmenopausal women: a meta-analysis, Osteoporos. Int. 26 (2015) 1605–1618.
[86] M. Martyn-St James, S. Carroll, Effects of different impact exercise modalities on bone mineral density in premenopausal women: a meta-analysis, J. Bone Miner. Metab. 28 (2010) 251–267.
[87] M. Martyn-St James, S. Carroll, A meta-analysis of impact exercise on postmenopausal bone loss: the case for mixed loading exercise programmes, Br. J. Sports Med. 43 (2009) 898–908.
[88] M. Martyn-St James, S. Carroll, Meta-analysis of walking for preservation of bone mineral density in postmenopausal women, Bone 43 (2008) 521–531.
[89] D.R. Carter, W.C. Hayes, The compressive behavior of bone as a two-phase porous structure, J. Bone Joint Surg. Am. 59 (1977) 954–962.
[90] E.F. Morgan, H.H. Bayraktar, T.M. Keaveny, Trabecular bone modulus-density relationships depend on anatomic site, J. Biomech. 36 (2003) 897–904.
[91] W.S. Enns-Bray, H. Bahaloo, I. Fleps, O. Ariza, S. Gilchrist, R. Widmer, P. Guy, H. Pálsson, S.J. Ferguson, P.A. Cripton, B. Helgason, Material mapping strategy to improve the predicted response of the proximal femur to a sideways fall impact, J. Mech. Behav. Biomed. Mater. 78 (2018) 196–205.
[92] I. Fleps, P. Guy, S.J. Ferguson, P.A. Cripton, B. Helgason, Explicit finite element models accurately predict subject-specific and velocity-dependent kinetics of sideways fall impact, J. Bone Miner. Res. 34 (2019) 1837–1850.
[93] K.M. Nicks, S. Amin, L.J. Melton III, E.J. Atkinson, L.K. McCready, B.L. Riggs, K. Engelke, S. Khosla, Three-dimensional structural analysis of the proximal femur in an age-stratified sample of women, Bone 55 (2013) 179–188.
[94] E. Schileo, E. Dall'Ara, F. Taddei, A. Malandrino, T. Schotkamp, M. Baleani, M. Viceconti, An accurate estimation of bone density improves the accuracy of subject-specific finite element models, J. Biomech. 41 (2008) 2483–2491.
[95] C.S. Rajapakse, A.R. Farid, D.C. Kargilis, B.C. Jones, J.S. Lee, A.J. Johncola, A. S. Batzdorf, S.S. Shetye, M.W. Hast, G. Chang, MRI-based assessment of proximal femur strength compared to mechanical testing, Bone 133 (2020), 115227.
[96] C.M. Phan, M. Matsuura, J.S. Bauer, T.C. Dunn, D. Newitt, E.M. Lochmueller, F. Eckstein, S. Majumdar, T.M. Link, Trabecular bone structure of the calcaneus: comparison of MR imaging at 3.0 and 1.5 T with micro-CT as the standard of reference, Radiology 239 (2006) 488–496.
[97] K. Chiba, A.J. Burghardt, M. Osaki, S. Majumdar, Heterogeneity of bone microstructure in the femoral head in patients with osteoporosis: an ex vivo HR-pQCT study, Bone 56 (2013) 139–146.
[98] G. Chang, S. Honig, R. Brown, C.M. Deniz, K.A. Egol, J.S. Babb, R.R. Regatte, C. S. Rajapakse, Finite element analysis applied to 3-T MR imaging of proximal femur microarchitecture: lower bone strength in patients with fragility fractures compared with control subjects, Radiology 272 (2014) 464–474.
[99] S. Mori, R. Harruff, W. Ambrosius, D.B. Burr, Trabecular bone volume and microdamage accumulation in the femoral heads of women with and without femoral neck fractures, Bone 21 (1997) 521–526.
[100] U. Hansen, P. Zioupos, R. Simpson, J.D. Currey, D. Hynd, The effect of strain rate on the mechanical properties of human cortical bone, J. Biomech. Eng. 130 (2008), 011011.
[101] W.S. Enns-Bray, S.J. Ferguson, B. Helgason, Strain rate dependency of bovine trabecular bone under impact loading at sideways fall velocity, J. Biomech. 75 (2018) 46–52.
[102] F. Feldman, S.N. Robinovitch, Reducing hip fracture risk during sideways falls: evidence in young adults of the protective effects of impact to the hands and stepping, J. Biomech. 40 (2007) 2612–2618.
[103] W.S. Enns-Bray, J.S. Owoc, K.K. Nishiyama, S.K. Boyd, Mapping anisotropy of the proximal femur for enhanced image based finite element analysis, J. Biomech. 47 (2014) 3272–3278.
[104] W.S. Enns-Bray, O. Ariza, S. Gilchrist, R.P. Widmer Soyka, P.J. Vogt, H. Palsson, S. K. Boyd, P. Guy, P.A. Cripton, S.J. Ferguson, B. Helgason, Morphology based anisotropic finite element models of the proximal femur validated with experimental data, Med. Eng. Phys. 38 (2016) 1339–1347.
[105] V. Komisar, S.N. Robinovitch, The role of fall biomechanics in the cause and prevention of bone fractures in older adults, Curr Osteoporos Rep. 19 (2021) 381–390.
[106] M. Nasiri Sarvi, Y. Luo, Sideways fall-induced impact force and its effect on hip fracture risk: a review, Osteoporos. Int. 28 (2017) 2759–2780.
[107] I. Fleps, W.S. Enns-Bray, P. Guy, S.J. Ferguson, P.A. Cripton, B. Helgason, On the internal reaction forces, energy absorption, and fracture in the hip during simulated sideways fall impact, PLoS One. 13 (2018), e0200952.